Neurobiology of Disease 124 (2019) 163–175

Contents lists available at ScienceDirect

Neurobiology of Disease

journal homepage: www.elsevier.com/locate/ynbdi

Portrait of blood-derived extracellular vesicles in patients with Parkinson's disease

Jérôme Lamontagne-Proulx[a], Isabelle St-Amour[a], Richard Labib[b], Jérémie Pilon[b], Hélèna L. Denis[a], Nathalie Cloutier[a], Florence Roux-Dalvai[a], Antony T. Vincent[c], Sarah L. Mason[d], Caroline Williams-Gray[d], Anne-Claire Duchez[a], Arnaud Droit[a,e], Steve Lacroix[a,e], Nicolas Dupré[a,f], Mélanie Langlois[a,f], Sylvain Chouinard[g], Michel Panisset[g], Roger A. Barker[d], Eric Boilard[a,h,*], Francesca Cicchetti[a,i,*]

[a] Centre de recherche du CHU de Québec, Québec, QC, Canada
[b] Département de mathématiques et génie industriel, École Polytechnique de Montréal, Montréal, QC, Canada
[c] Institut de Biologie Intégrative et des Systèmes, Université Laval, Québec, QC, Canada
[d] Department of Clinical Neurosciences, John van Geest Centre for Brain Repair, University of Cambridge, Cambridge, United Kingdom
[e] Département de médecine moléculaire, Université Laval, Québec, QC, Canada
[f] Département de médecine, Université Laval, Département de neurosciences, Hôpital de l'Enfant-Jésus, Québec, QC, Canada
[g] Centre Hospitalier de l'Université de Montréal and Centre de recherche du Centre Hospitalier de l'Université de Montréal, Hôpital Notre-Dame, Département de médicine, Université de Montréal, Montréal, QC, Canada
[h] Département de microbiologie-infectiologie et d'immunologie, Université Laval, Québec, QC, Canada
[i] Département de psychiatrie & neurosciences, Université Laval, Québec, QC, Canada

ARTICLE INFO

Keywords:
Blood cells
Erythrocytes
Extracellular vesicles
Alpha-synuclein

ABSTRACT

The production of extracellular vesicles (EV) is a ubiquitous feature of eukaryotic cells but pathological events can affect their formation and constituents. We sought to characterize the nature, profile and protein signature of EV in the plasma of Parkinson's disease (PD) patients and how they correlate to clinical measures of the disease. EV were initially collected from cohorts of PD (n = 60; Controls, n = 37) and Huntington's disease (HD) patients (Pre-manifest, n = 11; manifest, n = 52; Controls, n = 55) – for comparative purposes in individuals with another chronic neurodegenerative condition – and exhaustively analyzed using flow cytometry, electron microscopy and proteomics. We then collected 42 samples from an additional independent cohort of PD patients to confirm our initial results. Through a series of iterative steps, we optimized an approach for defining the EV signature in PD. We found that the number of EV derived specifically from erythrocytes segregated with UPDRS scores corresponding to different disease stages. Proteomic analysis further revealed that there is a specific signature of proteins that could reliably differentiate control subjects from mild and moderate PD patients. Taken together, we have developed/identified an EV blood-based assay that has the potential to be used as a biomarker for PD.

1. Introduction

The last few years of research has seen our understanding of Parkinson's disease (PD) change dramatically. One of the major breakthroughs has been the realization that PD is a heterogeneous disorder, which brings with it challenges for the development and identification of useful biomarkers for diagnosis and disease progression, as well as the ability to track the successful translation of novel treatments to the clinic. This new understanding of the different clinical profiles seen in populations of PD patients has begun to translate into a redefinition of PD, as is evidenced by new diagnostic criteria released by the International PD and Movement Disorder Society (MDS) (Berg et al., 2014). This task force has also pointed out the importance of identifying reliable biomarkers for clinico-pathological diagnoses. Indeed, the development of a biomarker that could serve as a diagnostic tool, and/or a dependable predictor of disease course and evolution

Abbreviations: EV, Extracellular vesicles; EEV, Extracellular vesicles derived from erythrocytes; LEDD, Levodopa equivalent daily dose; PD, Parkinson's disease; UPDRS, Unified Parkinson Disease Rating Scale

* Corresponding author at: Centre de Recherche du CHU de Québec, Axe Neurosciences, T2-07, 2705, Boulevard Laurier, Québec, QC G1V 4G2, Canada.
E-mail addresses: Eric.Boilard@crchudequebec.ulaval.ca (E. Boilard), Francesca.Cicchetti@crchudequebec.ulaval.ca (F. Cicchetti).

https://doi.org/10.1016/j.nbd.2018.11.002
Received 3 September 2018; Received in revised form 9 October 2018; Accepted 3 November 2018
Available online 05 November 2018
0969-9961/

(and thus stratify populations of patients) as well as to assess treatment efficacy is of critical importance and urgently needed.

The search for such biomarkers has recently included the investigation of extracellular vesicles (EV); small entities that carry intracellular molecules and which mediate cell-to-cell communication in both physiological and disease conditions (Quek and Hill, 2017). EV encompass entities such exosomes stored in multivesicular bodies and microvesicles derived from the plasma membrane. Based on the process dictating their release, EV are subdivided into three major groups: 1) exosomes are produced by exocytosis of multivesicular bodies (diameter ranges ≈50–150 nm), 2) microvesicles, also termed microparticles or ectosomes, are generated by cytoplasmic membrane budding and fission (diameter ranges ≈100–1000 nm) and 3) apoptotic bodies are released by apoptotic cells (diameter ranges > 1000 nm) (Marcoux et al., 2016). However, these definitions are still subject to change given the facts that 250 nm in size exosomes have been described, apoptotic cells can release exosome-like vesicles and there is no specific markers of EV subtypes (El Andaloussi et al., 2013; György et al., 2011b; van der Pol et al., 2016). The International Society of Extracellular Vesicles endorses EV as the term to use, as it more liberally encompasses all vesicle types released by cells (Lötvall et al., 2014).

EV are composed of membrane proteins and lipids, as well as cytoplasmic components of the cell from which they originate, such as mRNA and miRNA, organelles or infectious particles (e.g. prions, virus) (Boilard, 2018; Porro et al., 2015). Their protein cargo, cell signature and availability in bodily fluids make EV very attractive candidate biomarkers and have already been studied in the blood, cerebrospinal fluid (CSF), urine and brains of patients with PD (see Fig. S1) (Abd-Elhadi et al., 2015; Alvarez-Erviti et al., 2011; Araki et al., 2016; Barbour et al., 2008; Bartels et al., 2011; Danzer et al., 2012; El-Agnaf et al., 2006; Emmanouilidou et al., 2010; Fauvet et al., 2012; Fraser et al., 2013; Grey et al., 2015; Helferich et al., 2015; Ho et al., 2014; Kong et al., 2014; Kunadt et al., 2015; Melachroinou et al., 2013; Nakai et al., 2007; Nikam et al., 2009; Pretorius et al., 2014; Renella et al., 2014; Shi et al., 2014; Stuendl et al., 2016; Sudha et al., 2003; Tomlinson et al., 2015; Tsunemi et al., 2014; Wang et al., 2015). For example, EV derived from the CSF contain α-synuclein (α-Syn), its associated pathogenic species as well as the LRRK2 protein (Fraser et al., 2013). However, routinely collecting CSF presents a challenge given the invasive nature needed to collect it while plasma is a very accessible fluid that further allows real time monitoring, and which has consequently been more extensively studied from a biomarker perspective.

One of the reasons that EV have become attractive for biomarker development relates to advances in their isolation involving ultracentrifugation, centrifugation by density gradient, size exclusion using membranes and columns, polymeric precipitation, capture by immune-affinity and microfluidic approaches (Shevchenko et al., 1996). However, the bulk of the already published work on EV in bio-fluids relies on using a series of differential centrifugations with or without size filtration, for example gradient techniques that concentrate and purify EV (Konoshenko et al., 2018; Willis et al., 2017). Techniques utilizing solely the ultracentrifugation to perform EV counts are biased because they favor aggregations of vesicles while co-isolating a number of contaminants, such as proteins (Linares et al., 2015). Techniques to isolate EV have therefore recently been developed with the goal of maintaining the integrity and purity of the isolated entities (Konoshenko et al., 2018). We sought to use these advances to develop new approaches that would allow for the optimal analysis of EV in blood, and therefore shed light on a more accurate picture of these elements in PD with the hope that this could be used for biomarker development. This work initially involved optimizing the FACS analysis by stringent controls to unequivocally identify EV and their cell origin, performing test-retest experiments to validate consistency of results over time in the same patient and finally, using hemoglobin removal to uncover the entire proteome of EV analyzed. This having been done, we then sought to characterize the nature and profile of EV in the plasma of patients, and how they correlate to clinical measures of disease state as well as defining the protein content in the subpopulations of EV. Finally, we sought to validate this whole approach using a second independent cohort of patients with PD.

2. Materials and methods

2.1. Ethics statement and participant recruitment

Institutional review boards approved this study (CHU de Québec, #A13-2-1096; CHUM, #14.228; Cambridge Central Regional Ethics Committee, REC #03/303 & #08/H0306/26; and Cambridge University Hospitals Foundation Trust Research and Development department, R&D #A085170 & #A091246) in accordance with the Declaration of Helsinki, and written informed consents were obtained from all participants.

Blood samples were initially collected from 2 cohorts of patients with a total of 60 PD [one in Cambridge UK; one in Quebec Canada] as well as 37 age- and sex-matched healthy Controls (Table 1). For comparison, blood samples were also collected from a cohort of 52 Huntington's disease (HD) individuals [collected in Montreal, Canada] along with 55 age- and sex-matched healthy Controls (Table S1). Subsequently, an additional and independent cohort of 42 PD patients was collected to corroborate the results related to EV derived from erythrocyte (EEV) counts obtained from these first cohorts of patients (Table S3). In the case of PD patients, the UK Parkinson's Disease Society Brain diagnostic criteria were used, which gives a diagnostic accuracy of 98.6% when applied by movement disorder specialists (Hughes et al., 2002; Massano and Bhatia, 2012). The patients, at the time of bleeding, also underwent clinical evaluation which included the Unified Parkinson Disease Rating Scale (UPDRS), the Hoehn and Yahr (H&Y) scale, the Mini Mental State Examination (MMSE), the Addenbrooke's Cognitive Examination (ACE) and the Beck Depression Inventory (BDI). UPDRS was obtained from the UK and Montreal cohorts but not the Quebec cohort for logistical reasons. In the case of the HD patients, their Unified Huntington Disease Rating Scale (UHDRS), Total Functional capacity (TFC) and calculated values for burden of disease (BDS) were all collected at the time of venepuncture and their diagnosis was confirmed by genetic testing. Participants were further asked to fill out a questionnaire related to health issues and medication and a full blood count was performed in all patients on the day of blood sampling. Comorbidities were determined from medical information reported by the participant or caregiver. Cancer refers to a participant having suffered from any cancer in the past. Medications were converted into levodopa equivalent daily dose (LEDD) using common calculator tools. It should be noted that blood sampling was conducted by the same team of investigators, following identical procedures in both UK and Canada.

For the test-retest experiments, collection of blood samples was performed on 25 healthy individuals with 2 samples per subject, taken after a 2 h interval. This cohort included 11 men and 14 women with a mean age of 29 ± 5 years with no clinical reports of co-morbidities or medication intake. Note that fasting was not required prior to blood samplings in any of the cohorts that were recruited for this study. Calculation of coefficient of variation in percentage (%CV) of concentration measurements of EEV was performed using GraphPad PRISM® Version 6.0 (GraphPad Software, LaJolla, CA). CV is a measure of the dispersion of data points around the mean, i.e. a ratio of the standard deviation with the mean.

Given that 1) the material of blood tubes, 2) the extent of the time the samples were frozen and 3) the number of times the samples were frozen and thawed, are all recognized factors that may impact on reproducibility, we consistently used polypropylene tubes, quantification experiments were performed within 6 months of blood sampling and all samples related to one type of analysis were conducted on the same day and thawed for the same duration in the same conditions. Any of the samples were not frozen nor thawed more than twice.

Table 1
Participant clinical information – PD cohort. Disease severity as measured using the H&Y scale (score): Mild (1–1.5); Moderate (2–2.5); Severe (3–3.5). *$p < .05$ vs. CTRL. Statistical analyses were performed using a Kruskal Wallis test followed by Dunn's multiple comparison test. **Abbreviation**: ACE, Addenbrooke's Cognitive Examination; BDI, Beck Depression Inventory; CTRL, Control; H&Y, Hoehn and Yahr; MMSE, Mini-Mental State Examination; PD, Parkinson's disease; UPDRS, Unified Parkinson's Disease Rating Scale.

PD cohort						
	CTRL	PD Patients – Stages of disease				
		Unknown	Mild	Moderate	Severe	*p* value
n	37	7	12	33	8	
Age	66.8	69.8	66.7	71.1	75.0*	**0.04**
Gender F (M)	18 (19)	1 (6)	6 (6)	16 (17)	0 (8)	**0.05**
Disease severity						
Hoehn & Yahr (*n*)			1 ± 0.3 (12)	2 ± 0.2 (33)	3 ± 0.5 (8)	**<0.0001**
UPDRS (*n*)			38 ± 11 (6)	52 ± 19 (17)	73 ± 20 (6)	**0.02**
MMSE (*n*)			29 ± 2 (7)	29 ± 1 (19)	26 ± 3 (6)	**0.01**
BDI (*n*)			3 ± 2 (6)	4 ± 2 (17)	13 ± 7 (4)	**0.03**
ACE (*n*)			96 ± 4 (6)	92 ± 7 (17)	84 ± 14 (6)	0.13
Comorbidities						
Depression	3	1	2	1	2	0.29
Cancer	5	0	3	4	1	0.64
Diabetes	2	0	0	1	2	0.10
Hypertension	10	1	2	10	3	0.76
Hypercholesterolemia	5	0	1	6	1	0.73
Asthma	3	1	1	5	0	0.71
Allergies	2	0	2	6	2	0.28

2.2. Preparation of platelet-free plasma and EV labeling

Citrated blood (5 ml) was centrifuged twice for 15 min at 2500 *g* at room temperature (BD Vacutainer®, 369714). Platelet-free plasma (PFP) was harvested and stored at −80 °C within 2 h of sampling following previously published guidelines (Lacroix et al., 2012).

For all experiments, diluted annexin-V buffer (BD Pharmingen, Mississauga, ON, Canada) and phosphate buffered saline (PBS) were filtered on 0.22 µm pore size membranes (PALL, Mississauga, ON, Canada). To quantify EV according to their cell of origin, the following surface markers were used: CD235a + (erythrocytes) (5 µl), CD31 + / CD41- (endothelial cells) (1 µl), CD41 + (platelets) (5 µl), CD45 + (leukocytes) (3 µl), CD45 + CD14 + (monocytes) (10 µl) and CD45 + CD15 + (granulocytes) (2 µl). Given the recognized presence of phosphatidylserine on a proportion of blood EV (Boilard et al., 2015), fluorochrome-labeled annexin-V (5 µl), which avidly binds exposed phosphatidylserine, was also used as a labeling agent. PFP (5 µl) was incubated with Phenylalanyl-prolyl-arginyl Chloromethyl Ketone (PPACK) 10 mM (Calbiochem, Etobicoke, ON, Canada) for 5 min followed by a 30 min incubation with antibodies and annexin-V in a final PBS volume of 100 µl, all at room temperature. Finally, samples were diluted to a final volume of 2 ml prior to FACS analysis. The following antibodies were purchased from BD Pharmingen and used for all analyses: FITC-conjugated mouse anti-human CD235a (clone GA-R2 (HIR2), 1/20), PE-conjugated mouse anti-human CD31 (clone WM59, 1/100), V450-conjugated mouse anti-human CD41a (clone HIP8, 1/20), V450-conjugated mouse anti-human CD45 (clone HI30, 1/33), APC mouse anti-human CD14 (clone M5E2, 1/10), PE-conjugated mouse anti-human CD15 (clone HI98, 1/50), V450- and PerCP-Cy™5.5-conjugated annexin-V (1/20).

In all cases, the control samples came from healthy participants and the blood was collected on the same day as for the PD and HD patients in the UK and Canadian clinics. Every blood sample was processed immediately to avoid release of non-physiological EV. For analyses relating to EV in plasma, all blood samples were centrifuged twice at 2500 *g* to enable PFP recovery. The plasma was fractionated into 3 aliquots per individual and frozen immediately following processing (maximum of 2 h following blood sampling). Blood samples from Controls and PD were collected in parallel and laboratory analyses were blinded to participant status.

2.3. Flow cytometry quantification

For EV quantification, we used a FACS Canto II Special Order Research Product equipped with a forward scatter (FSC) coupled to a photomultiplier tube (FSC-PMT) and a small particle option. Flow cytometer performance tracking was carried out daily using the BD cytometer setup and tracking beads (BD Biosciences, San Jose, CA, USA). The size of the EV was determined using fluorescent silica beads of 100, 500 and 1000 nm (Fig. S2). The settings for the EV detection were determined as previously described using a threshold of 200 for SSC (also see Fig. S2) (Rousseau et al., 2015). The acquisition of EV was performed at low speed at an approximated rate of 10 µl/min. To determine background noise levels, antibody mixes were incubated in the absence of PFP sample and unlabeled PFP was used as a negative control. Every sample was re-identified to ensure that the experimenter was blind to clinical status.

2.4. Production and purification of EEV

Blood was collected in one 10 ml heparin tubes and centrifuged for 10 min at 282 *g* at room temperature (BD Vacutainer®, 367,880). Blood cells were washed first in PBS-2%FBS, then with 0.9% sodium chloride solution and centrifuged for 10 min at 750 *g*. To avoid leukocyte and/or platelet contamination, the buffy coat and upper fraction of erythrocytes were removed. To preserve erythrocytes, two volumes of glycerolyte 57 solution (57% glycerol, 142 mM sodium lactate, 1 mM KCl, 25 mM sodium phosphate pH 6.8) were added to the pellet and stored at −80 °C. For the in vitro generation of EEV, erythrocytes were thawed and EV production was induced, as previously described (Minetti et al., 2004).

For in vitro generation of EEV, 250 µl of erythrocytes were used, washed as previously described (Minetti et al., 2004) and erythrocyte pellet activated with 3 volumes of calcium ionophore solution (150 mM NaCl; 10 mM Tris-HCl; 1 mM CaCl2; 5 µM ionophore A23187 (Sigma, St Louis, MO)) for 30 min at 37 °C. Calcium ionophore is key to EV biogenesis. It

participates in the activation and inhibition of proteins and phospholipids at the cell membrane. Calcium ionophore A23187 induces a change in the concentration of calcium which leads to vesicle formation. In contrast to water and freezing, which are frequently used to provoke the release of EEV, calcium ionophores avoid the destruction of the erythrocyte membranes (Nguyen et al., 2016). The activation was stopped by the addition of 5 mM EDTA. Remaining erythrocytes were pelleted at 15000 g for 20 min. The EEV were centrifuged at 20000 *g* for 90 min and washed once in PBS. The EV pellet was re-suspended in lysis buffer (Thermo Scientific™, Pierce™ IP Lysis Buffer: 87788), proteins were quantified (90 µg per sample) and frozen at −80 °C until further analyses.

2.5. C-reactive protein, free hemoglobin and α-synuclein quantification

The concentrations of C-reactive protein (CRP) and free hemoglobin were determined in the PFP of all donors using the RayBio Human CRP ELISA Kit (RayBiotech, Norcross, GA, USA) and the hemolysis chart described by Zhao et al., 2012. To quantify α-Syn within erythrocytes and EEV, we used the human α-Syn ELISA kit (ThermoFisher Scientific, Waltham, MA, USA). Absorbance values were measured at 450 nm using a multi-detection microplate reader (Synergy HT; BioTek; Winooski, VT, USA). All ELISA tests were performed according to the manufacturer's instructions.

2.6. Scanning electron microscopy

For the visualization by scanning electron microscopy, EEV were prepared as previously described (Duchez et al., 2015). Preparations of erythrocytes (5 µl) were fixed in 2% paraformaldehyde and 2.5% glutaraldehyde in PBS buffer at least 24 h before standard dehydration. Samples were washed 3 times for 10 min with sodium cacodylate buffer (0.1 M, pH 7.3) and fixed with 1% osmium tetroxide in sodium cacodylate buffer for 90 min. Subsequently, samples were washed and processed in 50%, 70%, 90% and 100% EtOH for dehydration (10 min/step). Finally, samples were soaked in two subsequent baths of 100% EtOH, for 40 min and 10 min, air-dried overnight and coated with palladium. Observations were completed using a JEOL 6360LV scanning electron microscope (JEOL, Peabody, MA, USA).

2.7. Transmission electron microscopy

For transmission electron microscopy, EEV were prepared and observed, as previously described (Duchez et al., 2015). Preparations of EEV (30 µl) and activated erythrocytes (5 µl) were fixed in 2% paraformaldehyde at least 24 h before being dehydrated and sealed in LR white. Slices of LR white were placed on a Formvar/carbon-coated grid and processed for immunolabeling. The tissues mounted on grids were blocked in 0.5% BSA-c (Aurion, Wageningen, The Netherlands) in Hank's Balanced Salt Solution (HBSS) and incubated for 2 h with rabbit anti-α-Syn antibody (Abcam, Toronto, ON, Canada) or rabbit anti-α-Syn (phospho S129) antibody (Abcam, Toronto, ON, Canada), both diluted at 1:250 in HBSS and washed several times with distilled water. Finally, the grids were incubated for 60 min with an anti-rabbit IgG conjugated to 6 nm gold particles (EMS, Hatfield, PA, USA) diluted at 1:200, washed several times with distilled water and then fixed in 2.5% glutaraldehyde (EMS, Hatfield, PA, USA) in HBSS for 15 min. For this last step, the grids were treated with 3% uranyl acetate–0.075 M oxalate (pH 7.0) (EMS, Hatfield, PA, USA) for 1 min, which was followed by several washes in distilled water. All staining experiments included negative controls where the primary antibody was omitted from the incubation media. Observations were completed with a TECNAI Spirit G2 transmission electron microscope at 80 kV (FEI, Hillsboro, OR, USA).

2.8. Mass spectrometry analysis and label free protein quantification

The initial proteomic analyses were performed on 3 pools of 3 blood samples of each group. Following this, we undertook a completely new set of analyses to develop a method allowing us to isolate hemoglobin and better investigate the EEV proteome. For this, EV from an additional 4 individuals per group (Control, mild PD and moderate PD) were prepared as described above. For each individual, 25 µg of the protein sample, according to Bradford protein assay, was migrated onto an electrophoresis gel 4–12% Bis-Tris to separate hemoglobin from higher proteins. Following gel staining using Sypro Ruby (Thermo Fischer Scientific), the 12 kDa band corresponding to the hemoglobin size was cut out and the remaining part of the gel further fractioned into 7 slices, exposed to trypsin digestion and peptide extraction on a MassPrep liquid handling robot (Waters, Milford, USA) according to the manufacturer's specifications and the protocol of Shevchenko et al. with the modifications suggested by Havlis et al. (Havlis et al., 2003; Shevchenko et al., 1996). The extracted peptides from the 7 slices of the same individual were pooled and analyzed by nanoLC-MS/MS. The excised hemoglobin gel slices were also analyzed in the same conditions. One µg of each individual sample was injected on a Dionex UltiMate 3000 nanoRSLC system (Thermo Scientific) equipped with a nanoviper Acclaim Pepmap100, C18, 3 µm, 75 µm × 50 cm column (Thermo Scientific) connected to the nanoelectrospray source of an Orbitrap Fusion mass spectrometer (Thermo Scientific). The peptides were eluted at 300 nl/min using an acetonitrile gradient of 90 min with the mass spectrometer operating in the Data Dependent Acquisition mode. Peptide masses were measured in MS spectra detected in the orbitrap at 120 K resolution. MSMS fragmentation spectra of peptides were generated by Higher energy Collisional Dissociation (HCD) and detected in the ion trap. Spectra of peptides were searched against a human protein database (Uniprot Complete Proteome, taxonomy *Homo sapiens* – 83,512 sequences) using the Andromeda search engine included in MaxQuant software version 1.5.5.1. (Cox and Mann, 2008). MaxQuant was also used to validate proteins and peptides at a 1% False Discovery Rate using a target/decoy database search as well as to undertake a Label Free Quantification of the identified proteins using the 'match between runs' option.

2.9. Statistical analyses

Initial statistical analyses (unpaired *t*-tests when data followed normal distribution according to Shapiro-Wilk test or Mann-Witney in cases of non-normality) compared the number of each type of blood cells (erythrocytes, platelets, leukocytes, neutrophils, monocytes, lymphocytes) in control groups and patients of all stages of the UK and the Canadian cohorts. Comparison between each type of EV from every cells, including erythrocytes, platelets, leukocytes, neutrophils, monocytes, lymphocytes and endothelial cells were performed using Two-Way ANOVA. This revealed no statistical differences between groups, allowing us to pool cohorts for subsequent analyses. Statistical analyses pertaining to EEV quantification were performed using *The Statistics and Machine Learning Toolbox* provided by MathWorks™ under MATLAB™ platform using the MATLAB®R2015a version. Results obtained include the scatter plots, classical least-square linear regressions, R-squared and *p* values, as well as Pearson's goodness-of-fit. Interval cut-off values were determined using a loop program developed in MATLAB™. Model diagnostics, including residual behaviour and homoscedastivity, were obtained using the same Toolbox. Further details on the statistical tests chosen are described directly in the result section. For α-Syn quantification, data were first tested for normality using the D'Agostino & Pearson normality test. Comparisons between groups were obtained by Mann-Whitney *U* test or Kruskal-Wallis ANOVA and performed using Prism 6.0 (GraphPad Software, LaJolla, CA). For proteomic analyses, the 'Intensity values' contained in the output 'proteingroup.txt' file of MaxQuant were used to quantify each identified protein in each individual sample. The values were normalized by the median of each column (all intensity values of proteins for one sample). The missing values were imputed with a noise value corresponding to the 1-

A

Blood cell quantification

Cell type	Units	CTRL n	CTRL Mean	CTRL SD	PD n	PD Mean	PD SD	p value
Erythrocytes	10^9/ml	35	4.75	0.61	56	4.56	0.47	**0.049**
Platelets	10^6/ml	35	235	44	56	217	50	0.083
Leukocytes	10^6/ml	35	6.91	1.62	56	6.53	1.97	0.347
Monocytes	10^6/ml	35	0.56	0.14	56	0.53	0.18	0.308
Granulocytes	10^6/ml	35	4.34	1.38	56	4.32	1.62	0.979

B

Cell-derived EV quantification

Cell type	Markers	Units	CTRL n	CTRL Mean	CTRL SEM	PD n	PD Mean	PD SEM	p value
Erythrocytes	**CD235a+PS-**	**10^3/µl**	**36**	**18.2**	**46.5**	**59**	**32.0**	**36.3**	**0.04**
	CD235a+PS+	10^3/µl	36	0.22	0.07	59	0.29	0.05	0.70
	CD235a+ total	**10^3/µl**	**36**	**18.4**	**47.0**	**59**	**32.3**	**36.7**	**0.04**
	EV CD235a+/erythrocyte		**34**	**0.0039**	**0.011**	**57**	**0.0069**	**0.008**	**0.03**
Platelets	CD41+PS-	10^3/µl	37	7.88	1.68	59	10.3	1.33	0.27
	CD41+PS+	10^3/µl	37	15.2	3.20	59	17.9	2.53	0.51
	CD41+ total	10^3/µl	37	23.1	4.62	59	28.2	3.66	0.38
	EV CD41+/platelet		35	0.106	0.021	57	0.125	0.016	0.49
Endothelial cells	CD31+CD41-PS-	10^3/µl	37	15.8	8.04	59	11.7	6.37	0.75
	CD31+CD41-PS+	10^3/µl	37	0.91	0.13	59	0.92	0.10	0.96
	CD31+CD41- total	10^3/µl	37	16.7	8.03	59	12.6	6.36	0.75
Leukocytes	CD45+ total	10^3/µl	37	10.4	2.21	59	13.8	1.75	0.26
Monocytes	CD45-CD14+PS-	10^3/µl	37	1.70	0.30	59	1.62	0.24	0.85
	CD45-CD14+PS+	10^3/µl	37	1.20	4.00	59	5.84	3.17	0.50
	CD45+CD14+PS-	10^3/µl	37	0.16	0.04	59	0.14	0.03	0.74
	CD45+CD14+PS+	10^3/µl	37	0.60	0.79	59	1.47	0.63	0.59
	CD14+ total	10^3/µl	37	3.66	4.88	59	9.06	3.87	0.60
	EV CD14+/monocyte		35	7.08	1.99	57	9.16	1.56	0.41
Granulocytes	CD45-CD15+PS-	10^3/µl	37	12.3	7.96	59	16.7	6.30	0.92
	CD45-CD15+PS+	10^3/µl	37	2.21	0.77	59	1.39	0.61	0.47
	CD45+CD15+PS-	10^3/µl	37	0.55	0.36	59	1.15	0.29	0.20
	CD45+CD15+PS+	10^3/µl	37	1.01	0.30	59	1.25	0.24	0.56
	CD15+ total	10^3/µl	37	16.0	8.83	59	20.6	6.99	0.91

Diagnostic value

C

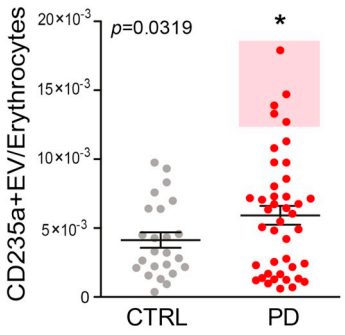

Fig. 1. A. Blood cell quantification. Full blood counts performed in PD patients (n = 57) revealed no significant differences in the total number of any cell type between patients and their respective healthy sex- and age-matched CTRL (n = 37), except for erythrocytes. Statistical analyses were performed using unpaired t-tests when data followed normal distributions according to the Shapiro-Wilk test or Mann-Witney in cases of non-normality. B. Cell-derived EV quantification. The quantification of EV in platelet-free plasma of PD patients and controls was performed by high-sensitivity flow cytometry. Phosphatidylserine was evaluated with Annexin V binding. The complete blood count was obtained at the time of blood sampling for 35/37 Controls and 57/59 PD and was used to calculate the EV per cell ratio. Statistical analyses were performed using a Two-Way ANOVA. * For erythrocyte-derived EV quantification, 1 outlier (determined using Grubbs' method with alpha = .0001) was removed. C. Diagnostic Value. Distribution plots of CD235a + EV/total number of erythrocytes between PD and healthy sex- and age-matched CTRL (PD, n = 42; CTRL, n = 24). Abbreviation: CD235a-45-41-31-15-14, cluster of differentiation; CTRL, Control; EV, extracellular vesicle; EEV, erythrocyte-derived extracellular vesicle; PD, Parkinson's disease; PS, phosphatidylserine; UPDRS, Unified Parkinson's Disease Rating Scale.

percentile of each sample column. For each comparison between two groups (Control, mild PD or moderate PD), proteins with too many imputed values where considered not quantifiable (a minimum of three not-imputed values in one of the 2 groups are required). A protein ratio was calculated between the two groups using the average of intensity values in each group. Finally, a statistical Welch's test was performed between the two groups. The protein ratios were transformed into log2(ratio) then centered by calculation of a z-score (z-score = (x - µ)/σ). A protein was considered as variant if it fulfilled the following criteria: minimum of 2 peptides quantified, Welch's test p value < .05 and absolute value of z-score > 1.96 (corresponding to values outside of the 95% confidence interval). The Gene Ontology enrichment analysis on the identified proteins was performed on the Cytoscape platform (v. 3.4.0) using the BinGO software version 3.0.3 against all human genes with GO annotation (Uniprot-GOA generated 2015-06-22) (Maere et al., 2005). Enrichment was calculated by a hypergeometric test and Bonferroni Family-Wise Error Rate (FWER) was used to correct for multiple testing. The data for the resulting 8 proteins was standardized, hierarchically clustered and visualized as a heatmap by using the statistical framework R (R Core Team, 2014). The robustness of the nodes was evaluated by computing Approximately Unbiased (AU) p values using the R package pvclust (10,000 bootstraps, average method and correlation-based dissimilarity matrix) (Suzuki and Shimodaira, 2006).

3. Results

3.1. Optimizing EV detection and reproducibility

While we performed EV analyses in plasma, we ensured that reproducibility of EV identification and labeling was robust. For this, we undertook a series of control experiments to properly set the EV gate and fluorescent silica beads of 100 nm (*Red*), 500 nm (*Blue*) and 1000 nm (*Yellow*) were acquired on a flow cytometer Canto II modified with a FSC-PMT small particle option (Fig. S2A-C). The acquisition was performed at low speed at an approximated rate of 10 µl/ml. The established EV gate was used for all experiments. Serial dilutions of EEV (1, 2, 4 and 10) were also undertaken to confirm the linearity of the quantification. FSC-PMT/SSC gates of PFP stained with annexin V fluorescent conjugate (a ligand of phosphatidylserine) and respective fluorochrome-conjugated antibodies directed against erythrocyte (CD235a+), endothelial (CD31+/CD41-), platelet (CD41+) and leukocyte (CD14+/CD45+, monocytes; CD15+/CD45+, granulocytes) derived EV were carefully established.

We further completed numerous controls to ensure specific EV labeling. We first determined that treatment with the ion chelator EDTA inhibited the binding of annexin V to phosphatidylserine. We observed minimal background using antibodies in the absence of PFP. Subsequently, EV sensitivity to 0.5% triton was assessed. Under these conditions, the membrane of the EV is dissolved while protein aggregates are left intact (György et al., 2011a). Results show that vast

majority of EV positive for their respective fluorochrome-conjugated antibodies were eliminated by detergent (Fig. S3A-C). Finally, we conducted a test-retest assay where two PFP samples per subject were collected approximately 2 h apart in 25 healthy individuals. All samples were tested in duplicate and minimal inter-sample variability was observed (16% ± 7%) (Fig. S4).

In addition to full blood count, and as a precautionary measure, hematocrit, mean corpuscular hemoglobin and mean corpuscular volumes were evaluated and showed similar values between groups (Fig. S5A). C-reactive protein quantifications were also obtained for all participants and revealed no differences between groups (Fig. S5B). We did, however, observe a significant increase in EEV concentration in the PFP of individuals with diabetes and those suffering, or having suffered, from cancer (data not shown) and thus these participants were excluded from our analyses. PFP samples with elevated free hemoglobin (using hemolysis chart), potentially due to hemolysis during blood sampling, were also excluded from further EEV-related analyses, which account for the small discrepancies between the total number of participants initially recruited and those reported in each analysis.

3.2. Increase in erythrocyte-derived EV in PD patients is not a diagnostic tool

Once all the controls were established and verified, we collected and carefully analyzed blood samples from patients with PD ($n = 60$) along with age/sex-matched healthy Controls ($n = 37$) (Table 1). Full blood counts were performed on each sample but did not reveal any differences in the number of platelets, leukocytes, monocytes, granulocytes except for erythrocytes, where a small significant difference ($p = .049$) was seen between PD patients and Controls (Fig. 1A). We then labeled each cell type as well as each EV population present in plasma to generate accurate counts of EV by FACS. A series of specific labelings highlighted a notable increase in the mean number of EEV in PD patients with respect to their age- and sex-matched healthy Controls ($p = .04$; Fig. 1B-C). None of the EV derived from the other blood cell populations showed differences between PD and Controls.

Based on this observation, we evaluated the diagnostic value of EV for PD by taking a closer look at the data distribution. However, this uncovered that only 5 patients were responsible for this significant difference (Fig. 1C, red inset). Further investigation, using a diagnostic accuracy test, revealed that the relevant proportion of the area under the Receiver Operating Characteristic (ROC) curve was .508 (data not shown), implying that the number of EEV could not be used as a discriminant between PD patients and healthy Controls. This was also confirmed by performing a Bayesian analysis of the data demonstrating that the proposed predictor of the onset of PD would be correct in < 1% of the cases (data not shown). We obtained a similar result when we separated the patients into mild and moderate states according to their UPDRS scores or by cohort (data not shown).

3.3. EV counts and clinical features

Despite the absence of a diagnostic difference in EEV counts, we explored whether there could be a relationship between the number of EEV and clinical measures such as H&Y stage, BDI, MMSE and ACE, but we found no significant correlations (data shown for H&Y, Fig. 2A). However, preliminary analyses revealed a correlation of $R^2 = .37$ with a p value of .0056 when plotting EEV counts/erythrocytes according to the UPDRS clinical rating scales (Fig. 2B). In depth statistical analyses further revealed intriguing, but striking correlations between the number of vesicles derived from the erythrocytes of PD patients and their total UPDRS (Fig. 2C). Statistical linear regression analysis was performed for each group and the R^2 values obtained demonstrated that in both cases, at least 87% of the variation in the total number of EEV/erythrocytes was due to the variation of the UPDRS (Fig. 2C). Moreover, the results were significant with respect to the p values obtained for each fit as they fell below the 5% confidence level. This could not be accounted for by medication, as there was no correlation with the patients LEDD (Fig. 2D-E). Importantly, these results were then corroborated in an independent cohort of 42 PD patients where the correlations yielded an $R^2 = .05$ and a p value of .15 when plotting EEV counts/erythrocytes against scores obtained with the UPDRS clinical rating scale (Fig. S6A). These results further validate, in a second cohort, that EEV counts allow to segregate groups of patients by severity of disease using the UPDRS scores (Mild: $R^2 = .7881$; $p = .0444$; Moderate: $R^2 = .5142$; $p < .0001$; Severe: $R^2 = .4929$; $p = .0236$, Fig. S6B-D). Moreover, these observations confirm that EEV levels do not correlate with medication (Fig. S6E-F).

In contrast to PD, correlation analyses failed to reveal an association between the number of EEV and HD stage using the UHDRS score (Fig. S7) (Denis et al., 2018).

3.4. Proteomic signature of EEV in PD

Given that these correlations are based on a small number of patients (cohort 1; $n = 19$ and cohort 2; $n = 42$), we sought to corroborate these results by examining the specific protein signature of EEV from mild and moderate PD patients (with respect to their UPDRS scores) and age-matched Controls. Given the significant amounts of hemoglobin within erythrocytes that could mask the true nature of the protein signature in EEV, we performed a label free quantitative proteomic analysis by nanoLC/MSMS (Wither et al., 2016) using two distinct approaches: with and without hemoglobin (Fig. 3A-B). By removing hemoglobin, we identified a total of 818 proteins in comparison with 356 when we did not undertake this methodological step (refer to Table S4 for complete list of proteins) – a modification which is clearly needed to give a much more accurate evaluation of the protein content of EEV. Additionally, a Gene Ontology enrichment analysis on the 'Cellular Component' ontology on the two sets of identified proteins in comparison with the whole human proteome, revealed that our samples are enriched with elements associated with 'vesicles' and 'hemoglobin complex' (Fig. S8).

Out of the 818 proteins identified in the proteome of EEV, 8 had expressions that were significantly different in patients with various stages of PD (Fig. 4A). Hierarchical clustering, coupled to a heatmap, allowed us to group individuals according to stages of disease (Control, mild PD and moderate PD) and provided compelling evidence that the 8 proteins identified could also be grouped into three categories. Proteins of group I were highly and predominantly expressed in Controls, proteins of group II were highly and predominantly expressed in mild PD patients and proteins belonging to group III were highly and predominantly expressed in moderate PD patients (Fig. 4B). This data set was further confirmed by volcano plots (Fig. 5).

Finally, we assessed whether α-Syn – which is not only a prominent component of Lewy bodies, one of the main pathological hallmark of PD, but is highly expressed in most blood cells – was differentially expressed in normal vs. diseased conditions. For this, we opted to use scanning electron microscopy, but this did not reveal any morphological changes between resting and activated erythrocytes in either condition (Fig. 6A). We further used transmission electron microscopy to quantify the number of EEV containing α-Syn and phosphorylated (serine 129) forms of the protein, but again there were no significant differences between PD patients and age- and sex-matched healthy Controls (Fig. 6B-C). Quantified α-Syn levels in EEV from PD patients and Controls using commercial ELISA kits corroborated these results (Fig. 6D).

4. Discussion

The primary goal of our study was to provide an accurate description of EV in PD patients. In order to do this, we took into account all relevant technical parameters and refined a number of approaches that

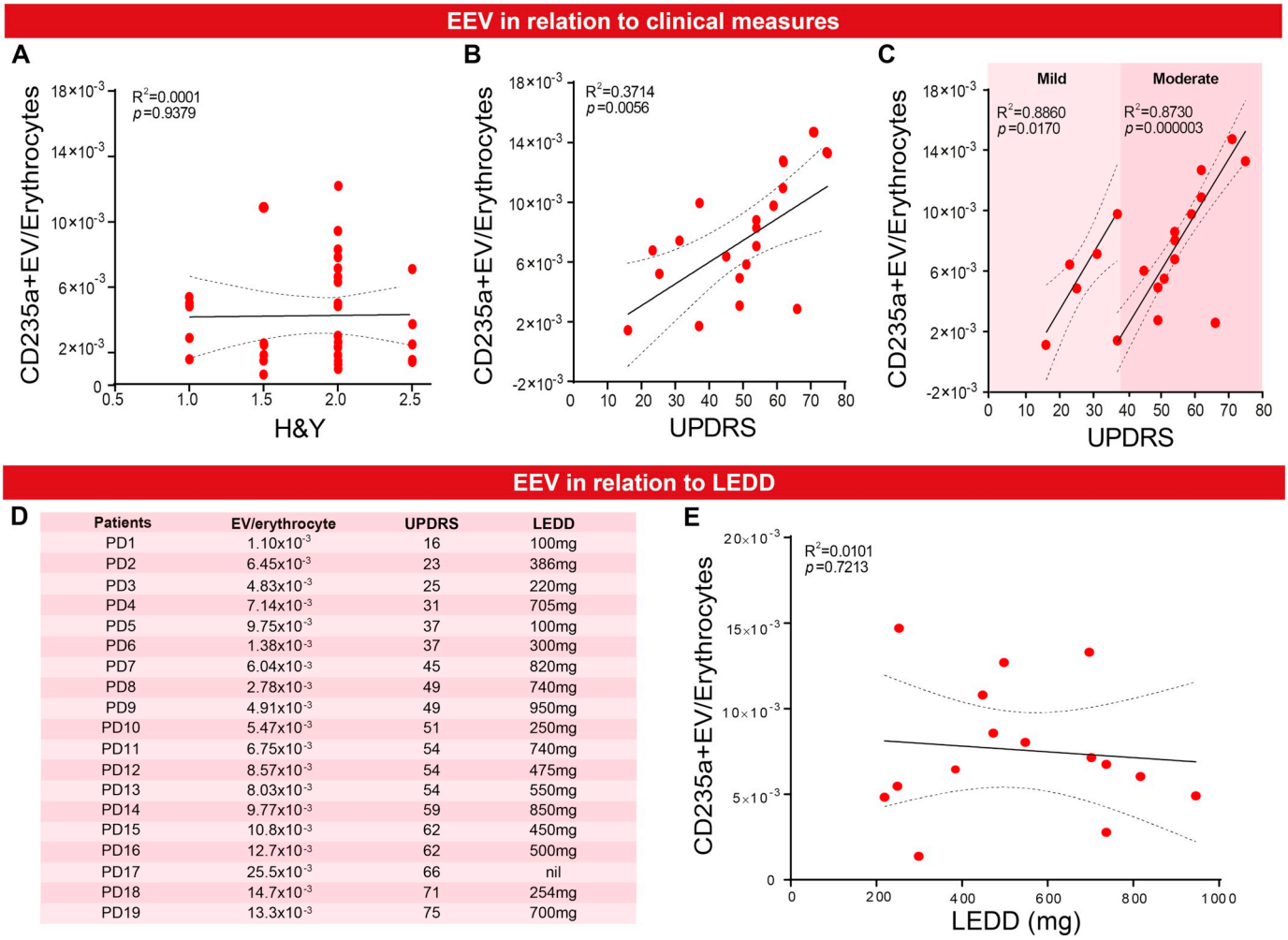

Patients	EV/erythrocyte	UPDRS	LEDD
PD1	1.10x10^{-3}	16	100mg
PD2	6.45x10^{-3}	23	386mg
PD3	4.83x10^{-3}	25	220mg
PD4	7.14x10^{-3}	31	705mg
PD5	9.75x10^{-3}	37	100mg
PD6	1.38x10^{-3}	37	300mg
PD7	6.04x10^{-3}	45	820mg
PD8	2.78x10^{-3}	49	740mg
PD9	4.91x10^{-3}	49	950mg
PD10	5.47x10^{-3}	51	250mg
PD11	6.75x10^{-3}	54	740mg
PD12	8.57x10^{-3}	54	475mg
PD13	8.03x10^{-3}	54	550mg
PD14	9.77x10^{-3}	59	850mg
PD15	10.8x10^{-3}	62	450mg
PD16	12.7x10^{-3}	62	500mg
PD17	25.5x10^{-3}	66	nil
PD18	14.7x10^{-3}	71	254mg
PD19	13.3x10^{-3}	75	700mg

Fig. 2. Relationship between EEV and clinical measures of PD. A. Absence of correlations between EEV/Erythrocyte counts and H&Y stage. B. Correlations between EEV/Erythrocyte counts with total UPDRS scores. C. Robust correlations between the number of EEV/total number of erythrocytes and UPDRS scores (PD, n = 19, from the UK cohort exclusively since the Quebec cohort did not have recent UPDRS scores available). D. EV/erythrocytes ratios, UPDRS scores and LEDD values for all PD patients used in the correlation analyses. E. Absence of correlation between the number of EEV and LEDD. Correlations reported were determined using Pearson's coefficient. Abbreviation: CD235a, glycophorin A; CTRL, Control; EEV, erythrocyte-derived extracellular vesicle; H&Y, Hoehn and Yahr; LEDD, Levodopa equivalent daily dose; PD, Parkinson's disease; UPDRS, Unified Parkinson's Disease Rating Scale.

may have been contentious in previous publications. These technical improvements included: 1) better methods to clearly identify EV when using FACS; 2) specific labeling to determine, with precision, the cell origin of the EV; 3) the demonstration of minimal test-retest variability intra-patient; 4) the deletion of hemoglobin from the samples for proteomic analyses which, as suspected, revealed numerous proteins which currently remain unidentified and finally, 5) the development of a user-friendly test which has the potential to be easily performed by western blots or other convenient quantitative proteomic approaches in any laboratory contexts using small quantities of blood. Once we had established the protocols for EV characterization, the second objective of this study was to explore the potential biomarker value of EV in PD. We found that EEV counts did map to disease stage, a finding that was corroborated by a unique protein signature in control subjects, mild and moderate PD patients. Our observations were then confirmed in a second independent cohort of PD patients, showing that our findings are robust and thus could have widespread applicability for helping stage PD patients in the future.

Blood counts were systemically performed in all patients, EV identification was replicated using the most accepted and standardized methods of repetition, stringent controls (microbeads, antibodies negative control, EDTA and Triton) (Rousseau et al., 2015) and complex combinations of antibodies which allowed for the specific labeling of vesicles. Standard techniques used to analyze EV (e.g. ultracentrifugation followed by immunoblotting) requires several days and a considerable amount of cells to isolate EV. However, quantification by flow cytometry takes only 1 day and requires a relatively small quantity of plasma (Konoshenko et al., 2018). We further demonstrated minimal test-retest variability. Sequential analyses of EV during the same day from the same individual/sample (intra-assay variation) has been reported to vary between 1 and 12% (Vestad et al., 2017). For example, circadian rhythm has been reported to influence the activation of platelets (Scheer et al., 2011) and therefore could influence the number of EV derived from these cells. In recent studies, counts of microvesicles derived from platelets across different flow cytometry platforms showed an inter-laboratory variability ranging between 28% and 37% (Vogel et al., 2016). In our hands, variability measures ranged between 1 and 30%, with an average at 16% ± 7%, indicative of strong reproducibility.

While proteomic studies of EEV have been previously reported, their description was limited to 270 proteins (Bosman et al., 2008, 2012). We herein report on an improved method to perform this type of analyses in blood samples by removing hemoglobin; a large protein that can easily mask others within a protein signature. Indeed, the high dynamic

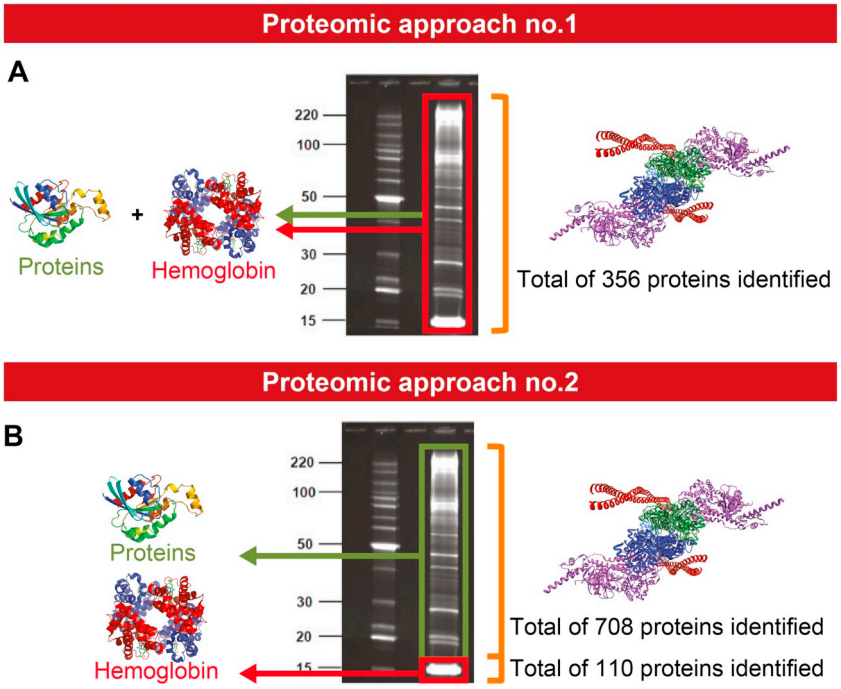

Fig. 3. A-B. Proteomic analyses with and without hemoglobin. To ensure the specificity of the protein signature detected in EEV, we performed proteomic analyses using two distinct methodologies. A. The first set of analyses by nanoLC-MS/MS and Label Free Quantification was performed on the complete proteome of the EEV, yielding 356 proteins. B. The second set of analyses was also performed on the entire EEV proteome but this time, isolating hemoglobin and quantifying the proteins present in both fractions. This approach uncovered 708 proteins in the EEV proteome with an additional 110 proteins in the hemoglobin fraction for a total of 818 proteins, indicating that removing hemoglobin provides a much more accurate evaluation of the protein content of EEV.

range of protein concentrations in erythrocytes and their EEV, due to the abundance of hemoglobin, decreases the capacity of the mass spectrometer to detect signals corresponding to low abundance proteins. Analyzing hemoglobin separately from proteins of other molecular weights, allowed us to go deeper into the EEV proteome, identifying 129% more proteins than in the initial analysis. It is important to reiterate that our proteomic analyses were performed using very stringent parameters, which included a minimum of 2 peptides per protein and p values of $< .05$ with an absolute z score of 1.96, corresponding to values outside of the 95% confidence range. Finally, our volcano plots and heatmap analyses revealed high specificity of the identified proteins for each group with nodes ranging between 80 and 90%. With this, reproducibility of our proteomics data is high despite the smaller sample size (analyses performed on 3 pools of 3 samples per group and subsequently on 4 individual samples per group). Reports of the role of these proteins in PD are rare. However of interest, QDPR has been reported to be essential to the bisosynthesis of norepinephrin and serotonin (Kaufman et al., 1975). ABHD14B have been shown to be dysregulated in mice following a levo-dopa treatment (Charbonnier-Beaupel et al., 2015) and mRNA for CNRIP1 are diminished in the striatum of a rat model of PD (Zeng et al., 1999). Finally, genetic variants of USP24 are associated to PD risk factors (Li et al., 2006) while another study of blood genetic profile revealed that ATP5A1 is downregulated in idiopathic PD patients (Shamir et al., 2017).

A recent report has also described that exosomes expressing α-Syn, which account for a subpopulation of EV, correlate with the UPDRS motor scores of PD patients (Shi et al., 2014). However, in this study, the authors examined exosomes from plasma and did not distinguish from which cell type they originated. We analyzed EV from all blood cells with significant results for a specific cell type: EV derived from erythrocytes. The biomarker that they suggested further relied on the presence of α-Syn, whereas our biomarker relies on the number of EV derived from erythrocytes and protein signature. In fact, we have identified a whole new set of proteins that seem to correlate with disease stages. Despite these differences, our data does support the main findings reported by Shi and colleagues (Shi et al., 2014) as well as corroborating those of others (Tomlinson et al., 2015) demonstrating that the concentration of α-Syn is not different in healthy subjects and PD patients.

Although staging of PD is often done using the H&Y clinical scale, we sought to use the UPDRS given its more comprehensive coverage of disease features – an approach that has recently been validated (Martínez-Martín et al., 2015). Using these scores in our initial study, we found that mild PD patients – with a UPDRS score lower than 37 – have an increased number of EV (correlations = .886); and that the exact same pattern then repeats itself with patients who had UPDRS scores between 37 and 75 (correlations = .873) with a marked resetting of the number of EV between these two stages. In this study, which was undertaken using patients in research clinics, patients with advanced disease (> 75 UPDRS) were not recruited in large numbers because they have difficulty making it to the clinics. In order to further validate this finding, we undertook a second study in another 42 patients with PD, which also included patients with more advanced disease. In this additional independent cohort, we demonstrated that we obtain similar results as in the first cohort. Namely, mild patients fell between the UPDRS scores of 0–39, moderate patients between 29 and 57 and severe patients (which we did not analyze in the first cohort), between 57 and 74 and that their EV changes paralleled that which we saw in our initial study. The overlapping zone between stages is likely due to a number of factors including the fact that 1) this new cohort was scored by a different clinician than our first cohort. Indeed, despite the fact that neurologists are trained to score patients in a similar fashion, the UPDRS remains a subjective measure that can vary between clinicians, even when they are been validated as a rater using the MDS training videos. 2) The FACS sorting apparatus we use to quantify EEV does generate a small percentage of variability (around 8%) between runs (data not shown). 3) We opted to test patients ON medication. It is therefore possible that the patient tested in the morning, who has just recently taken his/her medicine, scores slightly differently on the UPDRS than the patient who has taken his/her medications in the morning but is assessed late afternoon.

The bi-modal distribution revealed by the correlation analysis is intriguing but it would be very difficult to establish a definite cut-off between groups. The UPDRS is based on a questionnaire of > 70 different questions which are all based on a subjective assessment of the patient. A patient falling at the border of mild and moderate stage PD may be very difficult to categorize. We have already ruled out medication (in particular LEED) and a number of co-morbidities (depression, cancer, diabetes, hypertension, hypercholesterolemia, asthma,

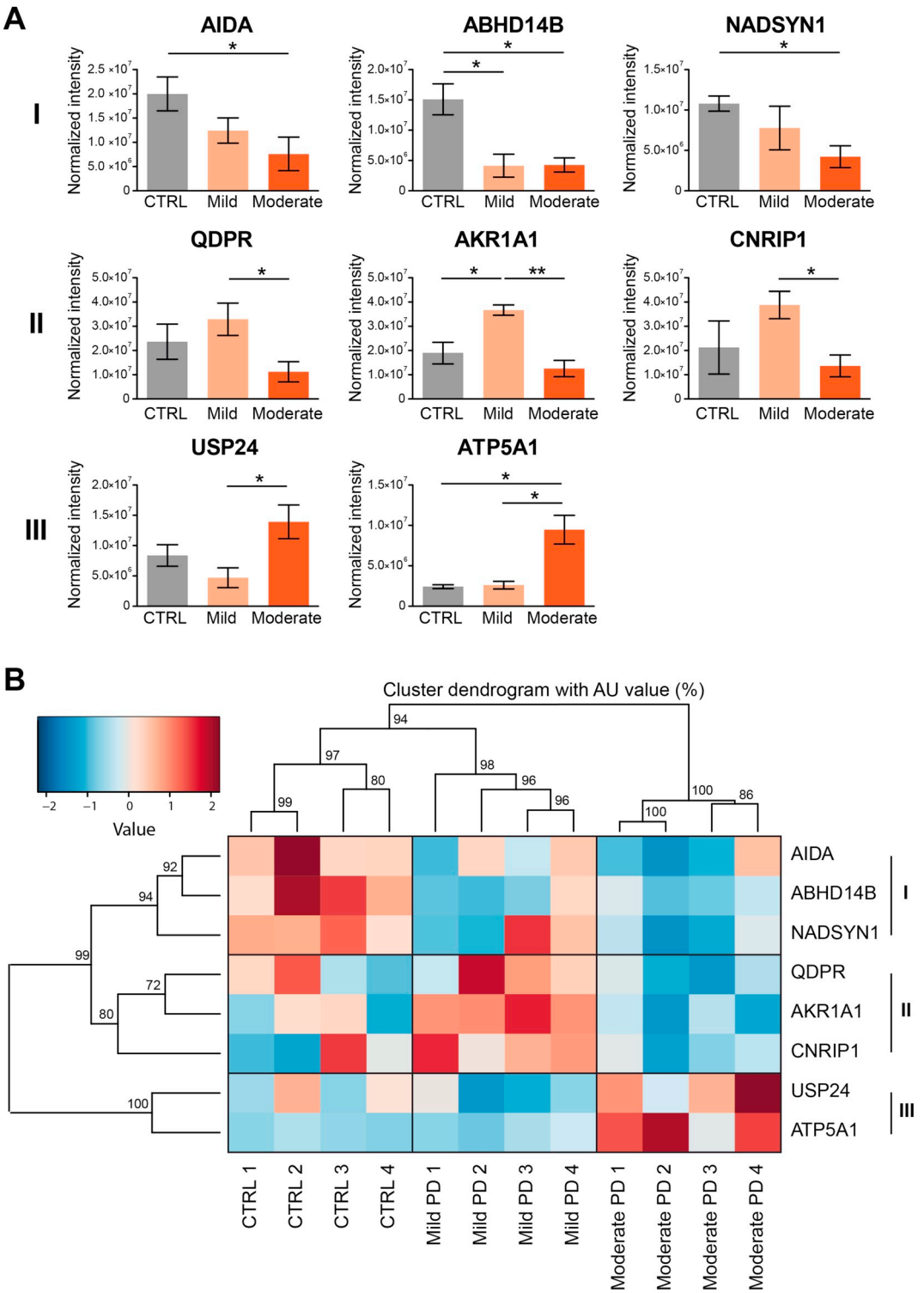

Fig. 4. A-B. Specific protein signature of EEV in PD patients. A. NanoLC-MS/MS Label-free analysis of EEV in PD patients and healthy age-matched CTRL revealed a total of 818 proteins, of which 8 had an expression that was significantly different as a function of PD stage. The proteins/genes have been further separated into 3 groups in relation to their variations in comparison to CTRL (Group I), mild PD (Group II) or moderate PD (Group III). B. Heatmap establishing correlations between disease stages and the abundance of the variable proteins. Cold and hot colours represent low and high correlation levels, respectively. Changes in protein levels were determined by Welch's test p value < 0.05 and $*p < .05$, $**p < .01$. Abbreviations: ABHD14B, alpha/beta hydrolase domain-containing protein 14B; AIDA, axin interactor dorsalization-associated protein; AKR1A1, alcohol dehydrogenase NADP+; ATP5A1, ATP synthase subunit alpha mitochondrial; CNRIP1, cannabinoid receptor-interacting protein 1; CTRL: Control; NADSYN1, glutamine-dependent NAD(+) synthetase; USP24, ubiquitin carboxyl-terminal hydrolase 24; PD, Parkinson's disease; QDPR, Quinoid Dihydropteridine Reductase.

allergies) as contributing to this. It is important to note that, while the R^2 values are significant, the samples used for each group (cohort 1; $n = 19$ and cohort 2; $n = 42$) are undersized with respect to the classical Pearson's chi-squared test. Further investigation with a larger cohort should therefore achieve more confident results, which we are doing now.

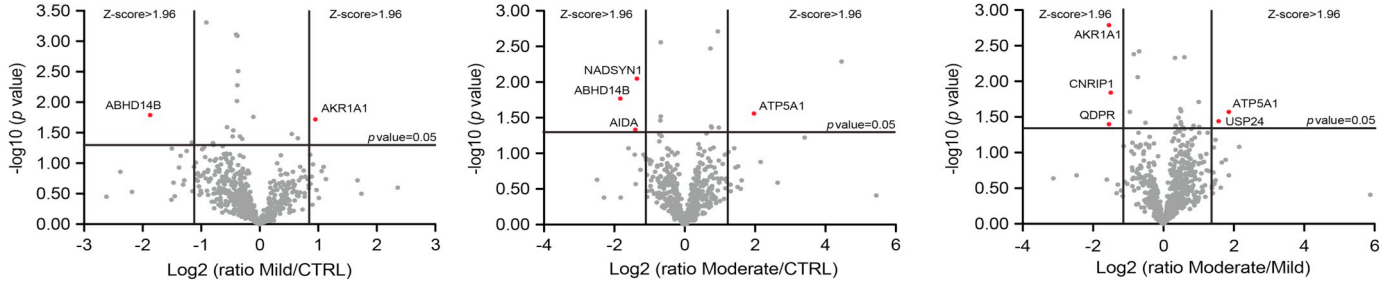

Fig. 5. Confirmation of EEV proteins selectively modified in PD patients by Volcano plots. The protein ratios (log2(ratio)) of the three comparison (mild PD/CTRL, moderate PD/CTRL and moderate PD/mild PD) were plotted over the corresponding Welch's test *p* value ($-\log10(p\text{-value})$). The graphs display a V shape, as expected, and only the proteins falling outside the limits of a *p* value < .05 and absolute value of z-score > 1.96 (identified by black lines) were considered as variant proteins (red dots). Two variant proteins were excluded given that they were quantified using only one peptide. Abbreviations: ABHD14B, alpha/beta hydrolase domain-containing protein 14B; AIDA, axin interactor dorsalization-associated protein; AKR1A1, alcohol dehydrogenase NADP+; ATP5A1, ATP synthase subunit alpha mitochondrial; CNRIP1, cannabinoid receptor-interacting protein 1; CTRL: Control; NADSYN1, glutamine-dependent NAD(+) synthetase; USP24, ubiquitin carboxyl-terminal hydrolase 24; QDPR, Quinoid Dihydropteridine Reductase.

5. Conclusion

Our study shed light on a potential biomarker indicative of disease stage, which is derived from 2 measures: the number of EEV/erythrocytes and the expression of 8 different proteins. The biological reasons as to why we find these correlations is still unresolved as is the pathological significance of the identified protein signature. Nevertheless, our findings are robust, reproducible and unveil a new biomarker with considerable potential for the stratification of patients, for instance. While the EEV counts used a particular type of flow cytometer that is not necessarily accessible to all laboratories, the identification of specific proteins that match clinical stages of PD implies that these could be more easily tested/detected in samples using simple and less expensive techniques yet to develop. Indeed, once the proteins have

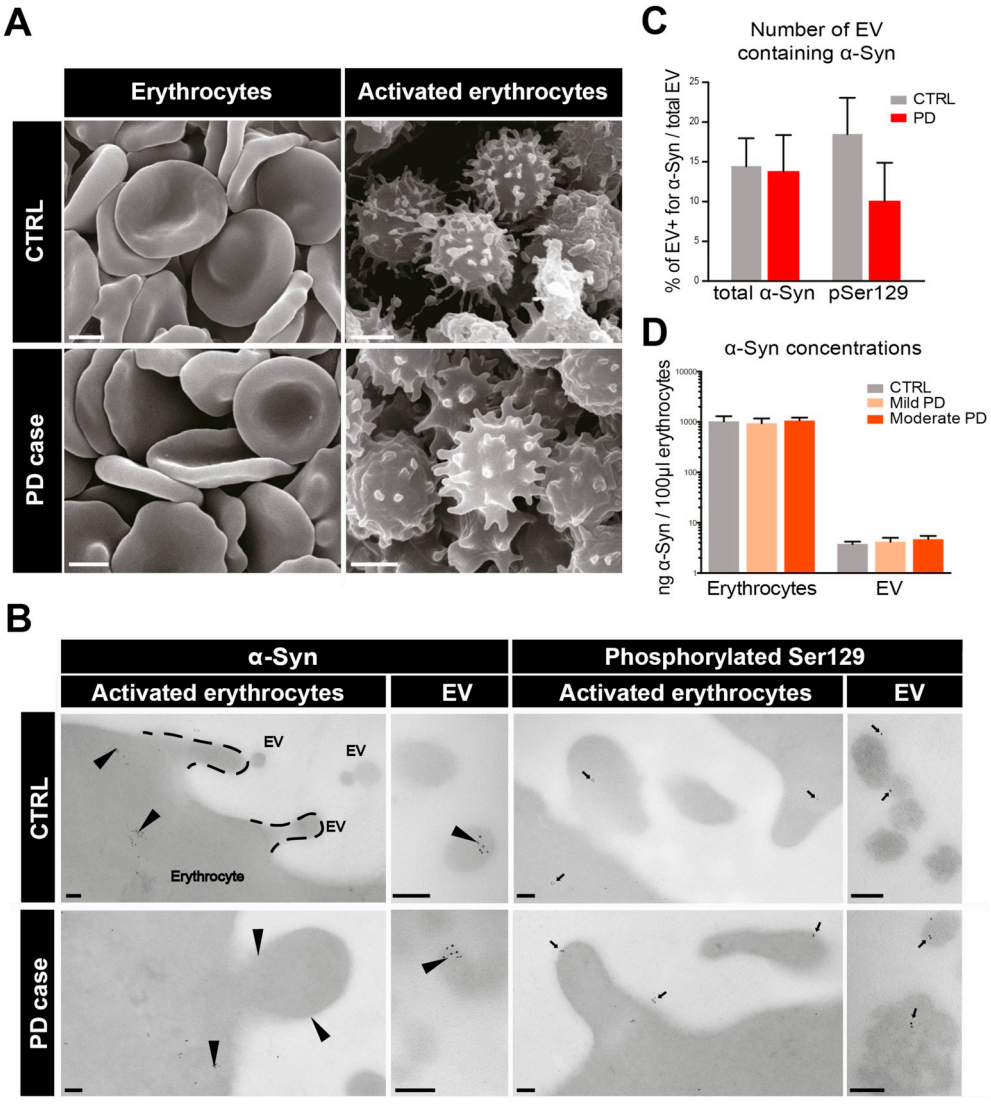

Fig. 6. Detection of normal and phosphorylated α-Syn in EEV. A. Representative scanning electron photomicrographs of resting and activated erythrocytes in both PD patients and healthy sex- and age-matched CTRL. Scale bar: 2 µm. B. Representative transmission electron microscopy images of immunogold labeling for α-Syn and α-Syn pS129 in activated erythrocytes and EEV (some examples delineated by dotted lines). Arrowheads point to positive immunolabeling for either α-Syn or α-Syn pS129. Scale bar: 100 nm. C. Quantification of α-Syn in EEV as detected by transmission electron microscopy and expressed as the percentage of EEVs positive for α-Syn/total number of EEV in healthy sex- and age-matched CTRL and PD patients ($n = 100$ erythrocytes sampled in $n = 3$ CTRL and $n = 3$ PD). D. Quantification of α-Syn in EEV by ELISA assays in healthy sex- and age-matched CTRL, mild and moderate stage patients ($n = 4$ erythrocytes per group; $n = 13$ EEV per group) showed no measurable changes in α-Syn levels between PD and healthy sex- and age-matched CTRL. Statistical analyses were performed using a Mann-Whitney *U* test (C) or a Kruskal-Wallis test (D). Abbreviations: α-Syn, α-synuclein; α-Syn pS129, α-synuclein phosphorylated Serine 129; CTRL, Control; EEV, erythrocyte-derived extracellular vesicle; PD, Parkinson's disease.

been identified, it is easy to buy commercially available antibodies against these proteins and to include them in quantitative assays. If replicated in other studies, we would then have a biomarker that could be easily tested in any laboratories or clinical context. The ability to develop a biomarker that not only works as a diagnostic tool but a predictor of disease stages/course would represent a major breakthrough in the field, further opening up to new therapeutic opportunities.

Supplementary data to this article can be found online at https://doi.org/10.1016/j.nbd.2018.11.002.

Acknowledgements

The authors would like to thank all the students and staff who helped with the blood collections in Cambridge UK, Quebec City and Montreal, Mr. Richard Janvier for his very skilful electron microscopy preparation and analyses, Mr. Gilles Chabot for art work and the Bioimaging platform of the Infectious Disease Research Centre, funded by an equipment and infrastructure grant from the Canadian Foundation for Innovation, for the coordination of the project, we thank Mrs. Lynn Jean from the CHU de Montréal, and importantly, all patients and their families for being so generous with their time in participating in this study.

Author contributions

J.L.P. participated in the design of the experiments and all aspects of the study including blood drive, experiments, data analysis and interpretation as well as preparation of figures. He also helped write some sections of the manuscript.

I.S.-A. participated in the design of the experiments and blood drives, took part in some data analysis and interpretation.

R.L. elaborated the statistical analysis strategy, performed statistical analyses related to Fig. 2 and wrote part of the texts relating to the correlation results.

J.P. performed statistical analyses related to Fig. 2.

H.L.D. participated to blood drives, analysis of data as well as preparation of figures and experiments related to Fig. S4 and Fig. S6.

N.C. was involved in the original design of the flow cytometry experiments and participated in the blood drive in Cambridge.

F.R.-D. contributed to the design and analyses of the proteomic experiments, performed the nanoLC-MS/MS and the Free Label quantification and helped with the figure design and writing of methodological aspects of the manuscript.

A.T.V. helped with the proteomic analyses, generated Figs. 3,4,5 and wrote related methodological aspects of the manuscript.

S.L.M. helped with patient recruitment in Cambridge and participated in the preparation of blood drive in Cambridge.

C.W-G. helped with patient recruitment and assessment in Cambridge.

A-C.D. was involved in the design of electron microscopy experiments and performed related analyses.

A.D. contributed to the proteomic analyses and data interpretation.

S.L. had the initial idea to study EEV in HD, set up the collaboration and was involved in discussions pertaining to the study.

N.D. recruited patients – Quebec PD cohort.

M.L. recruited patients – Quebec PD cohort.

S.C. recruited patients – Montreal HD cohort.

R.A.B. helped in the recruitment of patients, participated in data interpretation and revised the manuscript.

E.B. initiated the study and was involved in the experimental design. He also revised the manuscript.

F.C. initiated the study and was involved in the experimental design. She supervised the project and wrote the manuscript.

Financial disclosure

F.C., E.B., S.L. and I.S.-A. have filed a patent on the use of EEV as a biomarker in PD. J.L.P., R.L., J.P., H.L.D., N.C., F.R.-D., A.T.V., S.L.M., C.W-G., A-C.D., A.D., S.L., N.D., M.L., S.C. and R.A.B. declare no conflicts of interest.

Funding sources

The study was funded by The Michael J. Fox foundation, the Parkinson Society Canada and the Weston Brain Institute to F.C. as main PI who is also a recipient of a Researcher Chair from the Fonds de Recherche du Québec en santé (FRQS) providing salary support and operating funds. I.S.-A. was supported by a CIHR-Huntington Society of Canada postdoctoral fellowship. R.B. and J.P. are supported by the Natural Science and Engineering Research Council of Canada (NSERC). R.A.B., S.L.M. and C.W-G. are supported by a National Institute for Health Research (NIHR) award of a Biomedical Research Center to the University of Cambridge and Addenbrooke's Hospital. RAB is an NIHR Senior Investigator. H.L.D holds a Desjardins scholarship from the Fondation du CHU de Québec and a graduate student award from Parkinson Society Canada. A.-C.D. is supported by the Fonds de Recherche des maladies Rhumatismales de l'Université Laval and the Canadian Arthritis Network. E.B. is supported by the Canadian Institutes of Health Research and NSERC. N.D. is also funded by CIHR and by Canadian Consortium on Neurodegeneration in Aging (CCNA).

References

Abd-Elhadi, S., Honig, A., Simhi-Haham, D., Schechter, M., Linetsky, E., Ben-Hur, T., Sharon, R., 2015. Total and Proteinase K-Resistant α-Synuclein Levels in Erythrocytes, Determined by their Ability to Bind Phospholipids, associate with Parkinson's Disease. Sci. Rep. 5, 11120. https://doi.org/10.1038/srep11120.

Alvarez-Erviti, L., Seow, Y., Schapira, A.H., Gardiner, C., Sargent, I.L., Wood, M.J.A., Cooper, J.M., 2011. Lysosomal dysfunction increases exosome-mediated alpha-synuclein release and transmission. Neurobiol. Dis. 42, 360–367. https://doi.org/10.1016/j.nbd.2011.01.029.

Araki, K., Yagi, N., Nakatani, R., Sekiguchi, H., So, M., Yagi, H., Ohta, N., Nagai, Y., Goto, Y., Mochizuki, H., 2016. A small-angle X-ray scattering study of alpha-synuclein from human red blood cells. Sci. Rep. 6, 30473. https://doi.org/10.1038/srep30473.

Barbour, R., Kling, K., Anderson, J.P., Banducci, K., Cole, T., Diep, L., Fox, M., Goldstein, J.M., Soriano, F., Seubert, P., Chilcote, T.J., 2008. Red blood cells are the major source of alpha-synuclein in blood. Neurodegener. Dis. 5, 55–59. https://doi.org/10.1159/000112832.

Bartels, T., Choi, J.G., Selkoe, D.J., 2011. α-Synuclein occurs physiologically as a helically folded tetramer that resists aggregation. Nature 477, 107–110. https://doi.org/10.1038/nature10324.

Berg, D., Postuma, R.B., Bloem, B., Chan, P., Dubois, B., Gasser, T., Goetz, C.G., Halliday, G.M., Hardy, J., Lang, A.E., Litvan, I., Marek, K., Obeso, J., Oertel, W., Olanow, C.W., Poewe, W., Stern, M., Deuschl, G., 2014. Time to redefine PD? Introductory statement of the MDS Task Force on the definition of Parkinson's disease. Mov. Disord. 29, 454–462. https://doi.org/10.1002/mds.25844.

Boilard, E., 2018. Extracellular vesicles and their content in bioactive lipid mediators: more than a sack of microRNA. J. Lipid Res. 59, 2037–2046. https://doi.org/10.1194/jlr.R084640.

Boilard, E., Duchez, A.-C., Brisson, A., 2015. The diversity of platelet microparticles. Curr. Opin. Hematol. 22, 437–444. https://doi.org/10.1097/MOH.0000000000000166.

Bosman, G.J., Lasonder, E., Luten, M., Roerdinkholder-Stoelwinder, B., Novotný, V.M.J., Bos, H., De Grip, W.J., 2008. The proteome of red cell membranes and vesicles during storage in blood bank conditions. Transfusion 48, 827–835. https://doi.org/10.1111/j.1537-2995.2007.01630.x.

Bosman, G.J., Lasonder, E., Groenen-Döpp, Y.A., Willekens, F.L., Werre, J.M., 2012. The proteome of erythrocyte-derived microparticles from plasma: new clues for erythrocyte aging and vesiculation. J. Proteomics 76, 203–210. https://doi.org/10.1016/j.jprot.2012.05.031.

Charbonnier-Beaupel, F., Malerbi, M., Alcacer, C., Tahiri, K., Carpentier, W., Wang, C., During, M., Xu, D., Worley, P.F., Girault, J.-A., Hervé, D., Corvol, J.-C., 2015. Gene expression analyses identify Narp contribution in the development of L-DOPA-induced dyskinesia. J. Neurosci. 35, 96–111. https://doi.org/10.1523/JNEUROSCI.5231-13.2015.

Cox, J., Mann, M., 2008. MaxQuant enables high peptide identification rates, individualized p.p.b.-range mass accuracies and proteome-wide protein quantification. Nat. Biotechnol. 26, 1367–1372. https://doi.org/10.1038/nbt.1511.

Danzer, K.M., Kranich, L.R., Ruf, W.P., Cagsal-Getkin, O., Winslow, A.R., Zhu, L., Vanderburg, C.R., McLean, P.J., 2012. Exosomal cell-to-cell transmission of alpha synuclein oligomers. Mol. Neurodegener. 7, 42. https://doi.org/10.1186/1750-1326-7-42.

Denis, H.L., Lamontagne-Proulx, J., St-Amour, I., Mason, S.L., Weiss, A., Chouinard, S., Barker, R.A., Boilard, E., Cicchetti, F., 2018. Platelet-derived extracellular vesicles in Huntington's disease. J. Neurol. 265, 2704–2712. https://doi.org/10.1007/s00415-018-9022-5.

Duchez, A.-C., Boudreau, L.H., Naika, G.S., Bollinger, J., Belleannée, C., Cloutier, N., Laffont, B., Mendoza-Villarroel, R.E., Lévesque, T., Rollet-Labelle, E., Rousseau, M., Allaeys, I., Tremblay, J.J., Poubelle, P.E., Lambeau, G., Pouliot, M., Provost, P., Soulet, D., Gelb, M.H., Boilard, E., 2015. Platelet microparticles are internalized in neutrophils via the concerted activity of 12-lipoxygenase and secreted phospholipase A2-IIA. Proc. Natl. Acad. Sci. U. S. A. 112, E3564–E3573. https://doi.org/10.1073/pnas.1507905112.

El Andaloussi, S., Mäger, I., Breakefield, X.O., Wood, M.J.A., 2013. Extracellular vesicles: biology and emerging therapeutic opportunities. Nat. Rev. Drug Discov. 12, 347–357. https://doi.org/10.1038/nrd3978.

El-Agnaf, O.M.A., Salem, S.A., Paleologou, K.E., Curran, M.D., Gibson, M.J., Court, J.A., Schlossmacher, M.G., Allsop, D., 2006. Detection of oligomeric forms of alpha-synuclein protein in human plasma as a potential biomarker for Parkinson's disease. FASEB J. 20, 419–425. https://doi.org/10.1096/fj.03-1449com.

Emmanouilidou, E., Melachroinou, K., Roumeliotis, T., Garbis, S.D., Ntzouni, M., Margaritis, L.H., Stefanis, L., Vekrellis, K., 2010. Cell-produced alpha-synuclein is secreted in a calcium-dependent manner by exosomes and impacts neuronal survival. J. Neurosci. 30, 6838–6851. https://doi.org/10.1523/JNEUROSCI.5699-09.2010.

Fauvet, B., Mbefo, M.K., Fares, M.-B., Desobry, C., Michael, S., Ardah, M.T., Tsika, E., Coune, P., Prudent, M., Lion, N., Eliezer, D., Moore, D.J., Schneider, B., Aebischer, P., El-Agnaf, O.M., Masliah, E., Lashuel, H.A., 2012. α-Synuclein in central nervous system and from erythrocytes, mammalian cells, and Escherichia coli exists predominantly as disordered monomer. J. Biol. Chem. 287, 15345–15364. https://doi.org/10.1074/jbc.M111.318949.

Fraser, K.B., Moehle, M.S., Daher, J.P.L., Webber, P.J., Williams, J.Y., Stewart, C.A., Yacoubian, T.A., Cowell, R.M., Dokland, T., Ye, T., Chen, D., Siegal, G.P., Galemmo, R.A., Tsika, E., Moore, D.J., Standaert, D.G., Kojima, K., Mobley, J.A., West, A.B., 2013. LRRK2 secretion in exosomes is regulated by 14-3-3. Hum. Mol. Genet. 22, 4988–5000. https://doi.org/10.1093/hmg/ddt346.

Grey, M., Dunning, C.J., Gaspar, R., Grey, C., Brundin, P., Sparr, E., Linse, S., 2015. Acceleration of α-synuclein aggregation by exosomes. J. Biol. Chem. 290, 2969–2982. https://doi.org/10.1074/jbc.M114.585703.

György, B., Módos, K., Pállinger, E., Pálóczi, K., Pásztói, M., Misják, P., Deli, M.A., Sipos, A., Szalai, A., Voszka, I., Polgár, A., Tóth, K., Csete, M., Nagy, G., Gay, S., Falus, A., Kittel, A., Buzás, E.I., 2011a. Detection and isolation of cell-derived microparticles are compromised by protein complexes resulting from shared biophysical parameters. Blood 117, e39–e48. https://doi.org/10.1182/blood-2010-09-307595.

György, B., Szabó, T.G., Pásztói, M., Pál, Z., Misják, P., Aradi, B., László, V., Pállinger, E., Pap, E., Kittel, A., Nagy, G., Falus, A., Buzás, E.I., 2011b. Membrane vesicles, current state-of-the-art: emerging role of extracellular vesicles. Cell. Mol. Life Sci. 68, 2667–2688. https://doi.org/10.1007/s00018-011-0689-3.

Havlis, J., Thomas, H., Sebela, M., Shevchenko, A., 2003. Fast-response proteomics by accelerated in-gel digestion of proteins. Anal. Chem. 75, 1300–1306. https://doi.org/10.1021/ac026136s.

Helferich, A.M., Ruf, W.P., Grozdanov, V., Freischmidt, A., Feiler, M.S., Zondler, L., Ludolph, A.C., McLean, P.J., Weishaupt, J.H., Danzer, K.M., 2015. α-Synuclein interacts with SOD1 and promotes its oligomerization. Mol. Neurodegener. 10, 66. https://doi.org/10.1186/s13024-015-0062-3.

Ho, D.H., Yi, S., Seo, H., Son, I., Seol, W., 2014. Increased DJ-1 in urine exosome of Korean males with Parkinson's disease. Biomed. Res. Int. 2014. https://doi.org/10.1155/2014/704678.

Hughes, A.J., Daniel, S.E., Ben-Shlomo, Y., Lees, A.J., 2002. The accuracy of diagnosis of parkinsonian syndromes in a specialist movement disorder service. Brain J. Neurol. 125, 861–870. https://doi.org/10.1093/brain/awf080.

Kaufman, S., Holtzman, N.A., Milstien, S., Butler, L.J., Krumholz, A., 1975. Phenylketonuria due to a deficiency of dihydropteridine reductase. N. Engl. J. Med. 293, 785–790. https://doi.org/10.1056/NEJM197510162931601.

Kong, S.M.Y., Chan, B.K.K., Park, J.-S., Hill, K.J., Aitken, J.B., Cottle, L., Farghaian, H., Cole, A.R., Lay, P.A., Sue, C.M., Cooper, A.A., 2014. Parkinson's disease-linked human PARK9/ATP13A2 maintains zinc homeostasis and promotes α-Synuclein externalization via exosomes. Hum. Mol. Genet. 23, 2816–2833. https://doi.org/10.1093/hmg/ddu099.

Konoshenko, M.Y., Lekchnov, E.A., Vlassov, A.V., Laktionov, P.P., 2018. Isolation of Extracellular Vesicles: General Methodologies and latest Trends. Biomed. Res. Int. 2018. https://doi.org/10.1155/2018/8545347.

Kunadt, M., Eckermann, K., Stuendl, A., Gong, J., Russo, B., Strauss, K., Rai, S., Kügler, S., Falomir Lockhart, L., Schwalbe, M., Krumova, P., Oliveira, L.M.A., Bähr, M., Möbius, W., Levin, J., Giese, A., Kruse, N., Mollenhauer, B., Geiss-Friedlander, R., Ludolph, A.C., Freischmidt, A., Feiler, M.S., Danzer, K.M., Zweckstetter, M., Jovin, T.M., Simons, M., Weishaupt, J.H., Schneider, A., 2015. Extracellular vesicle sorting of α-Synuclein is regulated by sumoylation. Acta Neuropathol. 129, 695–713. https://doi.org/10.1007/s00401-015-1408-1.

Lacroix, R., Judicone, C., Poncelet, P., Robert, S., Arnaud, L., Sampol, J., Dignat-George, F., 2012. Impact of pre-analytical parameters on the measurement of circulating microparticles: towards standardization of protocol. J. Thromb. Haemost. 10, 437–446. https://doi.org/10.1111/j.1538-7836.2011.04610.x.

Li, Y., Schrodi, S., Rowland, C., Tacey, K., Catanese, J., Grupe, A., 2006. Genetic evidence for ubiquitin-specific proteases USP24 and USP40 as candidate genes for late-onset Parkinson disease. Hum. Mutat. 27, 1017–1023. https://doi.org/10.1002/humu.20382.

Linares, R., Tan, S., Gounou, C., Arraud, N., Brisson, A.R., 2015. High-speed centrifugation induces aggregation of extracellular vesicles. J. Extracell. Vesicles 4, 29509. https://doi.org/10.3402/jev.v4.29509.

Lötvall, J., Hill, A.F., Hochberg, F., Buzás, E.I., Di Vizio, D., Gardiner, C., Gho, Y.S., Kurochkin, I.V., Mathivanan, S., Quesenberry, P., Sahoo, S., Tahara, H., Wauben, M.H., Witwer, K.W., Théry, C., 2014. Minimal experimental requirements for definition of extracellular vesicles and their functions: a position statement from the International Society for Extracellular Vesicles. J. Extracell. Vesicles 3, 26913. https://doi.org/10.3402/jev.v3.26913.

Maere, S., Heymans, K., Kuiper, M., 2005. BiNGO: a Cytoscape plugin to assess overrepresentation of gene ontology categories in biological networks. Bioinforma. Oxf. Engl. 21, 3448–3449. https://doi.org/10.1093/bioinformatics/bti551.

Marcoux, G., Duchez, A.-C., Cloutier, N., Provost, P., Nigrovic, P.A., Boilard, E., 2016. Revealing the diversity of extracellular vesicles using high-dimensional flow cytometry analyses. Sci. Rep. 6, 35928. https://doi.org/10.1038/srep35928.

Martínez-Martín, P., Rodríguez-Blázquez, C., Alvarez, Mario, Null Arakaki, T., Arillo, V.C., Chaná, P., Fernández, W., Garretto, N., Martínez-Castrillo, J.C., Rodríguez-Violante, M., Serrano-Dueñas, M., Ballesteros, D., Rojo-Abuin, J.M., Chaudhuri, K.R., Merello, M., 2015. Parkinson's disease severity levels and MDS-Unified Parkinson's disease rating scale. Parkinsonism Relat. Disord. 21, 50–54. https://doi.org/10.1016/j.parkreldis.2014.10.026.

Massano, J., Bhatia, K.P., 2012. Clinical approach to Parkinson's disease: features, diagnosis, and principles of management. Cold Spring Harb. Perspect. Med. 2, a008870. https://doi.org/10.1101/cshperspect.a008870.

Melachroinou, K., Xilouri, M., Emmanouilidou, E., Masgrau, R., Papazafiri, P., Stefanis, L., Vekrellis, K., 2013. Deregulation of calcium homeostasis mediates secreted α-synuclein-induced neurotoxicity. Neurobiol. Aging 34, 2853–2865. https://doi.org/10.1016/j.neurobiolaging.2013.06.006.

Minetti, G., Ciana, A., Balduini, C., 2004. Differential sorting of tyrosine kinases and phosphotyrosine phosphatases acting on band 3 during vesiculation of human erythrocytes. Biochem. J. 377, 489–497. https://doi.org/10.1042/BJ20031401.

Nakai, M., Fujita, M., Waragai, M., Sugama, S., Wei, J., Akatsu, H., Ohtaka-Maruyama, C., Okado, H., Hashimoto, M., 2007. Expression of alpha-synuclein, a presynaptic protein implicated in Parkinson's disease, in erythropoietic lineage. Biochem. Biophys. Res. Commun. 358, 104–110. https://doi.org/10.1016/j.bbrc.2007.04.108.

Nguyen, D.B., Ly, T.B.T., Wesseling, M.C., Hittinger, M., Torge, A., Devitt, A., Perrie, Y., Bernhardt, I., 2016. Characterization of Microvesicles Released from Human Red Blood Cells. Cell. Physiol. Biochem. 38, 1085–1099. https://doi.org/10.1159/000443059.

Nikam, S., Nikam, P., Ahaley, S.K., Sontakke, A.V., 2009. Oxidative stress in Parkinson's disease. Indian J. Clin. Biochem. 24, 98–101. https://doi.org/10.1007/s12291-009-0017-y.

Porro, C., Trotta, T., Panaro, M.A., 2015. Microvesicles in the brain: Biomarker, messenger or mediator? J. Neuroimmunol. 288, 70–78. https://doi.org/10.1016/j.jneuroim.2015.09.006.

Pretorius, E., Swanepoel, A.C., Buys, A.V., Vermeulen, N., Duim, W., Kell, D.B., 2014. Eryptosis as a marker of Parkinson's disease. Aging 6, 788–819. https://doi.org/10.18632/aging.100695.

Quek, C., Hill, A.F., 2017. The role of extracellular vesicles in neurodegenerative diseases. Biochem. Biophys. Res. Commun. 483, 1178–1186. https://doi.org/10.1016/j.bbrc.2016.09.090.

R Core Team, 2014. R: a language and environment for statistical computing. R Found. R Foundation for Statistical Computing, Vienna, Austria. http://www.R-project.org/.

Renella, R., Schlehe, J.S., Selkoe, D.J., Williams, D.A., Lavoie, M.J., 2014. Genetic deletion of the GATA1-regulated protein α-synuclein reduces oxidative stress and nitric oxide synthase levels in mature erythrocytes. Am. J. Hematol. 89, 974–977. https://doi.org/10.1002/ajh.23796.

Rousseau, M., Belleannee, C., Duchez, A.-C., Cloutier, N., Levesque, T., Jacques, F., Perron, J., Nigrovic, P.A., Dieude, M., Hebert, M.-J., Gelb, M.H., Boilard, E., 2015. Detection and quantification of microparticles from different cellular lineages using flow cytometry. Evaluation of the impact of secreted phospholipase A2 on microparticle assessment. PLoS One 10, e0116812. https://doi.org/10.1371/journal.pone.0116812.

Scheer, F.A.J.L., Michelson, A.D., Frelinger, A.L., Evoniuk, H., Kelly, E.E., McCarthy, M., Doamekpor, L.A., Barnard, M.R., Shea, S.A., 2011. The human endogenous circadian system causes greatest platelet activation during the biological morning independent of behaviors. PLoS One 6, e24549. https://doi.org/10.1371/journal.pone.0024549.

Shamir, R., Klein, C., Amar, D., Vollstedt, E.-J., Bonin, M., Usenovic, M., Wong, Y.C., Maver, A., Poths, S., Safer, H., Corvol, J.-C., Lesage, S., Lavi, O., Deuschl, G., Kuhlenbaeumer, G., Pawlack, H., Ulitsky, I., Kasten, M., Riess, O., Brice, A., Peterlin, B., Krainc, D., 2017. Analysis of blood-based gene expression in idiopathic Parkinson disease. Neurology 89, 1676–1683. https://doi.org/10.1212/WNL.0000000000004516.

Shevchenko, A., Wilm, M., Vorm, O., Mann, M., 1996. Mass spectrometric sequencing of proteins silver-stained polyacrylamide gels. Anal. Chem. 68, 850–858. https://doi.org/10.1021/ac950914h.

Shi, M., Liu, C., Cook, T.J., Bullock, K.M., Zhao, Y., Ginghina, C., Li, Y., Aro, P., Dator, R., He, C., Hipp, M.J., Zabetian, C.P., Peskind, E.R., Hu, S.-C., Quinn, J.F., Galasko, D.R., Banks, W.A., Zhang, J., 2014. Plasma exosomal α-synuclein is likely CNS-derived and increased in Parkinson's disease. Acta Neuropathol. 128, 639–650. https://doi.org/10.1007/s00401-014-1314-y.

Stuendl, A., Kunadt, M., Kruse, N., Bartels, C., Moebius, W., Danzer, K.M., Mollenhauer, B., Schneider, A., 2016. Induction of α-synuclein aggregate formation by CSF exosomes from patients with Parkinson's disease and dementia with Lewy bodies. Brain J. Neurol. 139, 481–494. https://doi.org/10.1093/brain/awv346.

Sudha, K., Rao, A.V., Rao, S., Rao, A., 2003. Free radical toxicity and antioxidants in Parkinson's disease. Neurol. India 51, 60–62.

Suzuki, R., Shimodaira, H., 2006. Pvclust: an R package for assessing the uncertainty in

hierarchical clustering. Bioinformatics 22, 1540–1542. https://doi.org/10.1093/bioinformatics/btl117.

Tomlinson, P.R., Zheng, Y., Fischer, R., Heidasch, R., Gardiner, C., Evetts, S., Hu, M., Wade-Martins, R., Turner, M.R., Morris, J., Talbot, K., Kessler, B.M., Tofaris, G.K., 2015. Identification of distinct circulating exosomes in Parkinson's disease. Ann. Clin. Transl. Neurol. 2, 353–361. https://doi.org/10.1002/acn3.175.

Tsunemi, T., Hamada, K., Krainc, D., 2014. ATP13A2/PARK9 regulates secretion of exosomes and α-synuclein. J. Neurosci. 34, 15281–15287. https://doi.org/10.1523/JNEUROSCI.1629-14.2014.

van der Pol, E., Böing, A.N., Gool, E.L., Nieuwland, R., 2016. Recent developments in the nomenclature, presence, isolation, detection and clinical impact of extracellular vesicles. J. Thromb. Haemost. 14, 48–56. https://doi.org/10.1111/jth.13190.

Vestad, B., Llorente, A., Neurauter, A., Phuyal, S., Kierulf, B., Kierulf, P., Skotland, T., Sandvig, K., Haug, K.B.F., Øvstebø, R., 2017. Size and concentration analyses of extracellular vesicles by nanoparticle tracking analysis: a variation study. J. Extracell. Vesicles 6, 1344087. https://doi.org/10.1080/20013078.2017.1344087.

Vogel, R., Coumans, F.A.W., Maltesen, R.G., Böing, A.N., Bonnington, K.E., Broekman, M.L., Broom, M.F., Buzás, E.I., Christiansen, G., Hajji, N., Kristensen, S.R., Kuehn, M.J., Lund, S.M., Maas, S.L.N., Nieuwland, R., Osteikoetxea, X., Schnoor, R., Scicluna, B.J., Shambrook, M., de Vrij, J., Mann, S.I., Hill, A.F., Pedersen, S., 2016. A standardized method to determine the concentration of extracellular vesicles using tunable resistive pulse sensing. J. Extracell. Vesicles 5, 31242. https://doi.org/10.3402/jev.v5.31242.

Wang, X., Yu, S., Li, F., Feng, T., 2015. Detection of α-synuclein oligomers in red blood cells as a potential biomarker of Parkinson's disease. Neurosci. Lett. 599, 115–119. https://doi.org/10.1016/j.neulet.2015.05.030.

Willis, G.R., Kourembanas, S., Mitsialis, S.A., 2017. Toward Exosome-based Therapeutics: Isolation, Heterogeneity, and Fit-for-Purpose Potency. Front. Cardiovasc. Med. 4, 63. https://doi.org/10.3389/fcvm.2017.00063.

Wither, M.J., Hansen, K.C., Reisz, J.A., 2016. Mass Spectrometry-based Bottom-up Proteomics: Sample Preparation, LC-MS/MS Analysis, and Database Query strategies. Curr. Protoc. Protein Sci. 86, 16.4.1–16.4.20. https://doi.org/10.1002/cpps.18.

Zhao, J., Kan, Q., Wen, J., Li, Y., Sheng, Y., Yang, Y., Wu, J., Zhang, S., 2012. Hemolysis of blood samples has no significant impact on the results of pharmacokinetic data. J. Bioequiv. Availab. 4, 82–85. https://doi.org/10.4172/jbb.1000117.

Zeng, B.Y., Dass, B., Owen, A., Rose, S., Cannizzaro, C., Tel, B.C., Jenner, P., 1999. Chronic L-DOPA treatment increases striatal cannabinoid CB1 receptor mRNA expression in 6-hydroxydopamine-lesioned rats. Neurosci. Lett. 276, 71–74. https://doi.org/10.1016/S0304-3940(99)00762-4.